Inorg. Chem. **2006**, *45*, 3774–3781

Inorganic Chemistry
Article

# Synthesis, Structure, and Properties of an Fe(II) Carbonyl [(PaPy$_3$)Fe(CO)](ClO$_4$): Insight into the Reactivity of Fe(II)–CO and Fe(II)–NO Moieties in Non-Heme Iron Chelates of N-Donor Ligands

**Raman K. Afshar,**[†] **Apurba K. Patra,**[‡] **Eckhard Bill,**[‡] **Marilyn M. Olmstead,**[§] **and Pradip K. Mascharak***[,†]

*Department of Chemistry and Biochemistry, University of California, Santa Cruz, California 95064, Max-Plank-Institut für Strahlenchemie, Stiftstrasse 34-36, D-45470 Müllheim an der Ruhr, Germany, and Department of Chemistry, University of California, Davis, California 95616*

Received January 5, 2006

An Fe(II) carbonyl complex [(PaPy$_3$)Fe(CO)](ClO$_4$) (**1**) of the pentadentate ligand *N*,*N*-bis(2-pyridylmethyl)amine-*N*-ethyl-2-pyridine-2-carboxamide (PaPy$_3$H, H is the dissociable amide proton) has been synthesized and structurally characterized. This Fe(II) carbonyl exhibits its $\nu_{\mathrm{CO}}$ at 1972 cm$^{-1}$, and its $^1$H NMR spectrum in degassed CD$_3$CN confirms its $S = 0$ ground state. The bound CO in **1** is not photolabile. Reaction of **1** with an equimolar amount of NO results in the formation of the $\{$Fe–NO$\}^7$ nitrosyl [(PaPy$_3$)Fe(NO)](ClO$_4$) (**2**), while excess NO affords the iron(III) nitro complex [(PaPy$_3$)Fe(NO$_2$)](ClO$_4$) (**5**). In the presence of [Fe(Cp)$_2$]$^+$ and excess NO, **1** forms the $\{$Fe–NO$\}^6$ nitrosyl [(PaPy$_3$)Fe(NO)](ClO$_4$)$_2$ (**3**). Complex **1** also reacts with dioxygen to afford the iron(III) $\mu$-oxo species [$\{$(PaPy$_3$)Fe$\}_2$O](ClO$_4$)$_2$ (**4**). Comparison of the metric and spectral parameters of **1** with those of the previously reported $\{$Fe–NO$\}^{6,7}$ nitrosyls **3** and **2** provides insight into the electronic distributions in the Fe(II)–CO, Fe(II)–NO, and Fe(II)–NO$^+$ bonds in the isostructural series of complexes **1**–**3** derived from a non-heme polypyridine ligand with one carboxamide group.

## Introduction

The binding of small molecules such as dioxygen (O$_2$),[1] carbon monoxide (CO),[2,3] nitric oxide (NO),[4,5] and hydrogen sulfide (H$_2$S)[6,7] to iron(II) centers in heme systems has gained much interest as the role of these small molecules in cellular pathways becomes more evident. Ferrous heme proteins, such as myoglobin, hemoglobin, and cytochrome P450, bind CO with binding constants of the order of 10$^8$. This binding constant is 200 times stronger than that of O$_2$ and stems from the back-bonding to $\pi$* orbitals that make this bond relatively strong.[4,8]

The interest in the biological implications of CO has led to the investigations of CO coordination to synthetic Fe(II) complexes derived from porphyrin derivatives[9−11] and non-porphyrin macrocyclic ligands.[12−16] Most of these octahedral Fe(II) CO complexes (carbonyls) contain highly delocalized

---

[*] To whom correspondence should be addressed.

[†] University of California, Santa Cruz.

[‡] Max-Planck Institut für Strahlenchemie.

[§] University of California, Davis.

(1) Momenteau, M.; Reed, C. A. *Chem. Rev.* **1994**, *94*, 659−698.

(2) (a) Barañano, D. E.; Ferris, C. D.; Snyder, S. H. *Trends Neurosci.* **2001**, *24*, 99−106. (b) Boehning, D.; Snyder, S. H. *Science* **2002**, *298*, 2339−2340.

(3) (a) Hartsfield, C. L. *Antioxid. Redox Signaling* **2002**, *4*, 301−307. (b) Watts, R. N.; Ponka, P.; Richardson, D. R. *Biochem. J.* **2003**, *369*, 429−440.

(4) Cheng, L.; Richter-Addo, G. B. In *The Porphyrin Handbook*; Kadish, K. M., Smith, K. M., Guilard, R., Eds.; Academic Press: New York, 2000; Vol. 4, pp 219−291.

(5) Møller, J. K. S.; Skibsted, L. H. *Chem. Rev.* **2002**, *102*, 1167−1178.

(6) (a) Kashiba, M.; Kajimura, M.; Goda, N.; Suematsu, M. *Keio. J. Med.* **2002**, *51*, 1−10. (b) Kimura, H.; Nagai, Y.; Umemura, K.; Kimura, Y. *Antioxid. Redox Signaling* **2005**, *7*, 795−803.

(7) (a) Silfa, E.; Almeida, M.; Cerda, J.; Wu, S.; López-Garriga, J. *Biospectroscopy* **1998**, *4*, 311−326. (b) Bailly, X.; Vinogradov, S. *J. Inorg. Biochem.* **2005**, *99*, 142−150.

(8) (a) Keyes, M.; Mizukami, H.; Lumry, R. *Anal. Biochem.* **1967**, *18*, 126−142. (b) Alben, J. O.; Caughey, W. S. *Biochemistry* **1968**, *7*, 175−183.

(9) Scheidt, R. W.; Haller, K. J.; Fons, M.; Mashiko, T.; Reed, C. A. *Biochemistry* **1981**, *20*, 3653−3657.

(10) Peng, S.-M.; Ibers, J. A. *J. Am. Chem. Soc.* **1976**, *98*, 8032−8036.

(11) (a) Salzmann, R.; Ziegler, C. J.; Godbout N.; McMahon, M. T.; Suslick, K. S.; Oldfield, E. *J. Am. Chem. Soc.* **1998**, *120*, 11323−11334. (b) Salzmann, R.; McMahon, M. T.; Godbout N.; Sanders, L. K.; Wojdelski, M.; Oldfield, E. *J. Am. Chem. Soc.* **1999**, *121*, 3818−3828.

(12) Vaska, L.; Yamaji, T. *J. Am. Chem. Soc.* **1971**, *93*, 6673−6674.

(13) (a) Goedken, V. L. Molin-Case, J.; Whang, Y.-A. *J. Chem. Soc., Chem. Commun.* **1973**, 337−338. (b) Goedken, V. L. Peng, S.-M.; Molin-Norris, J. Park, Y.-A. *J. Am. Chem. Soc.* **1976**, *98*, 8391−8400.

(14) McCandlish, L. E.; Santarsiero, B. D.; Rose, N. J.; Lingafelter, E. C. *Acta Crystallogr.* **1979**, *B35*, 3053−3056.

10.1021/ic060020n CCC: $33.50

dianionic tetradentate ligands and an exogenous $\sigma$ donor (i.e., acetonitrile, pyridine, hydrazine) trans to the CO ligand. Goedken and co-workers have synthesized the only square pyramidal Fe(II) carbonyl containing a dianionic tetraazamacrocyclic ligand.[13b] An Fe(II) carbonyl derived from the tetrapodal pentadentate amine ligand (N$_4$Py) that incorporates open-chain aliphatic amines has recently been reported by Grohmann and co-workers.[15] All these Fe(II) carbonyls have characteristic CO stretches ($\nu_{CO}$) that range from 1920 to 1980 cm$^{-1}$.[9−13,15] Some of the Fe(II) carbonyls derived from non-heme ligands are highly sensitive to dioxygen, and are oxidized immediately to Fe(III) species with concomitant loss of CO.[13b]

During the past few years, we have synthesized a series of Fe(II) and Fe(III) complexes of the type [LFeX]$^{n+}$ where LH = pentadentate polypyridine ligands containing one carboxamide group (H is the dissociable amide proton) and X = MeCN, Cl$^-$, NO$_2^-$, CN$^-$, N$_3^-$, and NO.[17−20] We have now synthesized the low-spin Fe(II) CO complex [(PaPy$_3$)Fe(CO)](ClO$_4$) (**1**) where PaPy$_3^-$ = deprotonated *N*,*N*-bis(2-pyridyl-methyl)amine-*N*-ethyl-2-pyridine-2-carboxamide in order to confirm the electronic description of the corresponding low-spin {Fe−NO}$^7$ nitrosyl [(PaPy$_3$)Fe(NO)](ClO$_4$) (**2**) reported by us in a previous account.[18b] In this paper, we report the synthesis, structure, and reactivities of the Fe(II) carbonyl **1**. The Enemark and Feltham notation of {Fe−NO}$^7$ (7 is the sum of the d electrons of iron and the single $\pi$* electron of NO)[21] used to describe **2** has been somewhat ambiguous since both the iron center and NO can lose or accept electrons. To gain more insight into the location of the single electron of NO in **2**, we have now compared the spectroscopic properties of **1** (a true Fe(II) species) with those of **2**. We have also included the corresponding low-spin {Fe−NO}$^6$ nitrosyl [(PaPy$_3$)Fe(NO)](ClO$_4$)$_2$ (**3**)[18] in such comparison to gain further insight into the electronic description of these {Fe−NO}$^n$ nitrosyls. The reactions of **1** with O$_2$ and NO are also reported.

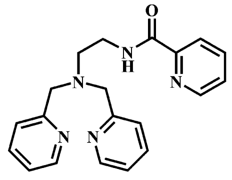

**PaPy$_3$H**

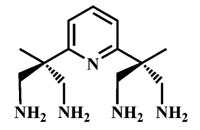

**N$_4$Py**

## Experimental Section

Ferrocenium tetrafluoroborate ([Fe(Cp)$_2$](BF$_4$)), acetonitrile (MeCN), methanol (MeOH), and triethylamine (Et$_3$N) were purchased from Aldrich Chemical Co., while CO gas was procured from Praxair. NO gas was purchased from Johnson Mathew Chemical Co. and was purified from higher oxides by passage through a long KOH column before use in reactions. The ligand PaPy$_3$H and the starting metal salts, [Fe(MeCN)$_4$](ClO$_4$)$_2$ and [Fe(DMF)$_6$](ClO$_4$)$_3$, were synthesized by following the published procedures.[17,22] All of the solvents were purified and/or dried by standard techniques and distilled prior to use. Standard Schlenk techniques were used during all syntheses to avoid exposure to dioxygen.

**Caution!** Transition metal perchlorates should be handled with great caution and be prepared in small quantities as metal perchlorates are hazardous and may explode upon heating.

**Synthesis of Compounds. [(PaPy$_3$)Fe(CO)](ClO$_4$) (1).** A solution of 0.120 g (0.35 mmol) of PaPy$_3$H and 0.038 g (0.38 mmol) of Et$_3$N in 30 mL of MeOH was thoroughly degassed by freeze−pump−thaw cycles. To the frozen MeOH solution of the ligand and base, a batch of 0.145 g (0.35 mmol) of solid [Fe(MeCN)$_4$](ClO$_4$)$_2$ was added and the frozen solution was warmed to room temperature in a 40 °C water bath. The dark red solution was stirred for 1 h at room temperature, and CO gas was bubbled into the solution for 5 min. The headspace of the Schlenk flask was then filled with CO, and the solution was placed at −20 °C for 48 h. Red-brown blocks were filtered and dried in vacuo (0.085 g, 46% yield). Anal. Calcd for C$_{25}$H$_{36}$ClFeN$_5$O$_{10}$ (**1**·4MeOH): C, 45.60; H, 5.52; N, 10.64. Found: C, 45.55; H, 5.58; N, 10.65. Selected IR frequencies (KBr disk, cm$^{-1}$): 3080 (w), 2938 (w), 2855 (w), 1972 ($\nu_{CO}$, s), 1633 ($\nu_{CO}$, s), 1601 (m), 1452 (m), 1405 (m), 1285 (w), 1091 ($\nu_{ClO4}$, s), 764 (m), 623 (m). Electronic absorption spectrum in MeCN, $\lambda_{max}$ (nm) ($\epsilon$ (M$^{-1}$ cm$^{-1}$)): 470 (4500), 390 (sh, 4480), 380 (sh, 4480). $^1$H NMR (500 MHz, CD$_3$CN, $\delta$ from TMS): 9.05 (d, 1H), 8.18 (m, 2H), 7.76 (t, 2H), 7.61 (m, 1H), 7.34 (d, 2H), 7.07 (t, 2H), 6.41 (d, 2H), 4.55 (dd, 4H, $J$ = 65 and 15 Hz), 3.27 (d, 2H), 3.11 (t, 2H). $^{13}$C NMR (125 MHz, CD$_3$CN, $\delta$ from TMS): 216, 163, 159, 152, 141, 140, 128, 126, 125, 123, 70, 67, 45.

**Reaction of 1 with O$_2$: Formation of [(PaPy$_3$)FeOFe(PaPy$_3$)](ClO$_4$)$_2$ (4).** A batch of 0.100 g (0.19 mmol) of [(PaPy$_3$)Fe(CO)](ClO$_4$) was dissolved in 15 mL of MeCN in the presence of dioxygen and stirred for 3 h. A portion of 25 mL of distilled Et$_2$O was added, and the solution was stored at −20 °C for 24 h. The red-orange blocks thus obtained of [(PaPy$_3$)FeOFe(PaPy$_3$)](ClO$_4$)$_2$ (**4**)[19] were filtered and washed with Et$_2$O and dried in vacuo (0.067 g, 70% yield). Selected IR frequencies (KBr disk, cm$^{-1}$): 3585 (m), 3079 (w), 2870 (w), 2284 (w), 1622 ($\nu_{CO}$, s), 1594 ($\nu_{CO}$, s), 1567 (s), 1486 (w), 1445 (m), 1399 (m), 1294(m), 1094 ($\nu_{ClO4}$, s), 784 ($\nu_{FeOFe}$, s), 624 (m). Electronic absorption spectrum in MeCN, ($\lambda_{max}$ (nm) ($\epsilon$ (M$^{-1}$ cm$^{-1}$)): 520 (sh, 2500), 430 (8790), 330 (11 800) 248 (30 650).

**Reaction of 1 with a Stoichiometric Amount of NO.** A batch of 0.100 g (0.19 mmol) of [(PaPy$_3$)Fe(CO)](ClO$_4$) was dissolved in 15 mL of a previously degassed solution of MeCN. Next, 4.3 mL (0.19 mmol) of NO gas was introduced to the reaction flask

---

(15) López, J. P.; Heinemann, F. W.; Prakash, R.; Hess, B. A.; Horner, O.; Jeandey, C.; Oddou, J.-L.; Latour, J.-M.; Grohmann, A. *Chem. Eur. J.* **2002**, *8*, 5709−5722.

(16) (a) Sellmann, D.; Blum, N.; Heinemann, F. W.; Hess, B. A. *Chem. Eur. J.* **2001**, *7*, 1874−1880. (b) Li, M.; Bonnet, D.; Bill, E.; Neese, F.; Weyhermuller, T.; Blum, N.; Sellman, D.; Wieghardt, K. *Inorg. Chem.* **2002**, *41*, 3444−3456.

(17) Rowland, J. M.; Olmstead, M. M.; Mascharak, P. K. *Inorg. Chem.* **2001**, *40*, 2810−2817.

(18) (a) Patra, A. K.; Afshar, R.; Olmstead, M. M.; Mascharak, P. K. *Angew. Chem. Int. Ed.* **2002**, *41*, 2512−2515. (b) Patra, A. K.; Rowland, J. M.; Marlin, D. S.; Bill, E.; Olmstead, M. M.; Mascharak, P. K. *Inorg. Chem.* **2003**, *42*, 6812−6823.

(19) Patra, A. K.; Afshar, R. K.; Rowland, J. M.; Olmstead, M. M.; Mascharak, P. K. *Angew. Chem. Int. Ed.* **2003**, *42*, 4517−4521.

(20) Afshar, R. K.; Patra, A. K.; Olmstead, M. M.; Mascharak, P. K. *Inorg. Chem.* **2004**, *43*, 5736−5743.

(21) Enemark, J. H.; Feltham, R. D. *Coord. Chem. Rev.* **1974**, *13*, 339−406.

(22) (a) Hodgkinson, J.; Jordan, R. B. *J. Am. Chem. Soc.* **1973**, *95*, 763−768. (b) Sugimoto, H.; Sawyer, D. T. *J. Am. Chem. Soc.* **1985**, *107*, 5712−5716.

via a gastight syringe. A previously degassed 25 mL portion of $Et_2O$ was then cannulated into the deep brown solution, and the reaction mixture was stored at −20 °C for 24 h. The dark brown-red blocks of $[(PaPy_3)Fe(NO)](ClO_4)$ (**2**) were filtered and washed with $Et_2O$ and dried in vacuo (0.065 g, 65% yield). Selected IR frequencies (KBr disk, $cm^{-1}$): 3072 (w), 2942 (w), 2860 (w), 2284 (w), 1613 ($\nu_{NO}$, s), 1590 ($\nu_{CO}$, s), 1454 (m), 1401 (w), 1373 (w), 1284(m), 1219 (w), 1085 ($\nu_{ClO4}$, s), 761 (m), 620 (m). Electronic absorption spectrum in MeCN, ($\lambda_{max}$ (nm) ($\epsilon$ ($M^{-1}$ $cm^{-1}$)): 830 (50), 476 (4300), 390 (sh, 3100), 370 (sh, 3200).

**$[(PaPy_3)Fe(NO)](ClO_4)_2$ (3) Method A. Conversion of 4 to 3.** A batch of 0.200 g (0.20 mmol) of $[(PaPy_3)FeOFe(PaPy_3)](ClO_4)_2$ and 0.095 g (0.42 mmol) of $Et_4NClO_4$ was dissolved in 25 mL of a thoroughly degassed solution of MeCN. Passage of purified NO gas to this red-orange solution caused a sharp color change to red. The reaction mixture was stirred for 1 h in the dark. Next, a 25 mL portion of $Et_2O$ was cannulated and the reaction mixture was stored at −20 °C for 24 h. The dark red crystals were filtered and washed with small portions of $Et_2O$ and dried in vacuo (0.15 g, 60% yield). Selected IR frequencies (KBr disk, $cm^{-1}$): 3082 (w), 2932 (w), 2867 (w), 1919 ($\nu_{NO}$, s), 1642 ($\nu_{CO}$, s), 1609 (m), 1453 (m), 1385 (m), 1289 (w), 1228 (w), 1090 ($\nu_{ClO4}$, s), 765 (m), 623 (m). Electronic absorption spectrum in MeCN, $\lambda_{max}$ (nm) ($\epsilon$ ($M^{-1}$ $cm^{-1}$)): 500 (1050), 365 (1850). $^1H$ NMR (500 MHz, $CD_3CN$, $\delta$ from TMS): 8.99 (d, 1H), 8.51 (t, 1H), 8.28 (d, 1H), 8.14 (t, 2H), 8.04 (m, 1H), 7.73 (d, 2H), 7.44 (t, 2H), 6.72 (d, 2H), 5.02 (dd, 4H), 3.73 (d, 2H), 3.68 (d, 2H).

**Method B. Conversion of 1 to 3.** A batch of 0.100 g (0.19 mmol) of $[(PaPy_3)Fe(CO)](ClO_4)$ and 0.051 g (0.19 mmol) of ferrocenium tetrafluoroborate were dissolved in 15 mL of a previously degassed solution of MeCN. The solution was stirred for 3 h, whereby an intense purple solution developed. Next, 0.043 g (0.19 mmol) of $Et_4NClO_4$ was added to the solution and purified NO gas was introduced to the solution for 5 min. The color of the solution changed to red. The red solution was stirred for an additional 2 h. The addition of 20 mL of distilled and degassed $Et_2O$ followed by subsequent cooling at −20 °C for 24 h afforded in dark red crystals of **3**. The dark crystals were filtered and washed with small portions of $Et_2O$ and dried in vacuo (0.054 g, 45% yield).

**$[(PaPy_3)Fe(NO_2)](ClO_4)$ (5).** We have previously reported this complex.[18] Here, two additional syntheses of the same complex are described. A solution of 0.300 g (0.86 mmol) of $PaPy_3H$ and 0.096 g (0.95 mmol) of $Et_3N$ in 25 mL of MeCN was thoroughly degassed by freeze−pump−thaw cycles. A batch of 0.0.360 g (0.86 mmol) of $[Fe(MeCN)_4](ClO_4)_2$ was added to the frozen solution, and the solution was allowed to warm to room temperature. Next, purified NO gas was bubbled into the dark red solution for 5 min and stirred for an additional 3 h. The color of the solution changed to reddish purple. A batch of 30 mL of $Et_2O$ was cannulated into the solution, and the mixture was stored at −20 °C for 24 h. The red blocks thus obtained were filtered and washed with small portions of $Et_2O$ and dried in vacuo (0.290 g, 61% yield). Selected IR frequencies (KBr disk, $cm^{-1}$): 3065 (w), 2958 (w), 2852 (w), 2249 (m), 1636 ($\nu_{CO}$, s), 1607 ($\nu_{CO}$, m), 1470 (m), 1446 (m), 1364 (s), 1280(m), 1090 ($\nu_{ClO4}$, s), 764 (m), 622 (m). Electronic absorption spectrum in MeCN, ($\lambda_{max}$ (nm) ($\epsilon$ ($M^{-1}$ $cm^{-1}$)): 512 (2700), 390 (sh, 2200), 340 (sh, 4100).

**Reactions of 1 with Excess NO: Conversion of 1 to 5.** A batch of 0.100 g (0.19 mmol) of $[(PaPy_3)Fe(CO)](ClO_4)$ was dissolved in 20 mL of a previously degassed solution of MeCN. Purified NO gas was introduced into the solution for 5 min, whereby the orange-red solution became dark red. Next, 20 mL of distilled and degassed $Et_2O$ was cannulated and the solution was cooled at −20 °C for 24 h. The red crystals were filtered and washed with small portions of $Et_2O$ and dried in vacuo (0.53 g, 51% yield).

**Table 1.** Summary of Crystal Data, Intensity Collection, and Structural Refinement Parameters for $[(PaPy_3)Fe(CO)](ClO_4)\cdot4MeOH$ (**1**·4MeOH)

| | |
|---|---|
| formula | $C_{25}H_{36}ClFeN_5O_{10}$ |
| molecular weight | 657.89 |
| cryst color, habit | red block |
| $T$, K | 90(2) |
| cryst syst | orthorhombic |
| space group | $P2_12_12_1$ |
| $a$, Å | 8.4679(3) |
| $b$, Å | 14.0642(6) |
| $c$, Å | 25.1370(10) |
| α, deg | 90 |
| $\beta$, deg | 90 |
| $\gamma$, deg | 90 |
| V, Å$^3$ | 2993.7 (2) |
| $Z$ | 4 |
| $d_{calcd}$, g $cm^{-3}$ | 1.460 |
| abs coeff, $mm^{-1}$ | 0.655 |
| GOF$^a$ on $F^2$ | 1.052 |
| R1$^b$ % | 0.0397 |
| wR2$^c$ % | 0.0910 |

[a] GOF = $[\sum w(F_o^2 - F_c^2)^2]/(M - N)^{1/2}$ ($M$ = no. of reflections, $N$ = no. of parameters refined). [b] R1 = $\sum||F_o| - |F_c||/\sum|F_c|$. [c] wR2 = $[[\sum w(F_o^2 - F_c^2)^2]/\sum w(F_o)^2]^{1/2}$.

**Table 2.** Selected Bond Distances (Å) and Bond Angles (deg) for $[(PaPy_3)Fe(CO)](ClO_4)\cdot4MeOH$ (**1**·4MeOH)

| | | | |
|---|---|---|---|
| Fe−N1 | 1.976(2) | Fe−C21 | 1.775(3) |
| Fe−N2 | 1.941(2) | C21−O2 | 1.153(4) |
| Fe−N3 | 1.997(2) | C6−O1 | 1.269(3) |
| Fe−N4 | 1.978(2) | C6−N2 | 1.299(4) |
| Fe−N5 | 1.993(2) | | |
| N1−Fe−N2 | 80.38(10) | N2−Fe−C21 | 175.07(12) |
| N1−Fe−N3 | 164.08(10) | N3−Fe−N4 | 84.17(10) |
| N1−Fe−N4 | 97.68(10) | N3−Fe−N5 | 82.25(10) |
| N1−Fe−N5 | 95.84(9) | N3−Fe−C21 | 98.29(11) |
| N1−Fe−C21 | 97.54(12) | N4−Fe−N5 | 166.31(10) |
| N2−Fe−N3 | 83.96(10) | N4−Fe−C21 | 89.35(11) |
| N2−Fe−N4 | 86.51(10) | N5−Fe−C21 | 90.96(11) |
| N2−Fe−N5 | 93.70(10) | Fe−C21−O2 | 176.5(3) |

**Physical Methods.** Absorption spectra were recorded on a Cary 50 Varian spectrophotometer. Samples were prepared in a $N_2$-filled glovebox. A Perkin-Elmer 1600 FTIR spectrophotometer was employed to monitor the infrared spectra. $^1H$ NMR and $^{13}C$ NMR spectra were recorded on a Bruker 500 MHz spectrometer at 298 K in $CD_3CN$. Mössbauer spectra were recorded with a conventional Mössbauer spectrometer operating in a constant acceleration mode and equipped with a $^{57}Co/Rh$ source at room temperature. The spectra were analyzed by a least-squares fit procedure using Lorentzian line shape. All isomer shift ($\delta$) and quadrupole splitting ($\Delta E_Q$) values are reported with respect to $^{57}Fe$-enriched metallic iron foil that was used for velocity calibration. Electrochemical measurements were performed with standard Princeton Applied Research instrumentation and a Pt-inlay electrode. Halfwave potentials ($E_{1/2}$) were measured versus aqueous saturated calomel electrode (SCE).

**X-ray Data Collection and Structure Solution and Refinement.** Reddish-orange blocks of **1**·4MeOH were obtained by storing a solution $[(PaPy_3)Fe(CO)](ClO_4)$ in MeOH under CO atmosphere at −20 °C for 24 h. Diffraction data were collected at 91 K on a Bruker SMART 1000 system. Mo Kα (0.710 73 Å) radiation was used, and the data were corrected for absorption. The structure was solved by direct methods (standard SHELXS-97 package). Machine parameters, crystal data, and data collection parameters for **1** are summarized in Table 1, while selected bond distances and angles are listed in Table 2. Complete crystallographic data for $[(PaPy_3)$-

**Scheme 1**

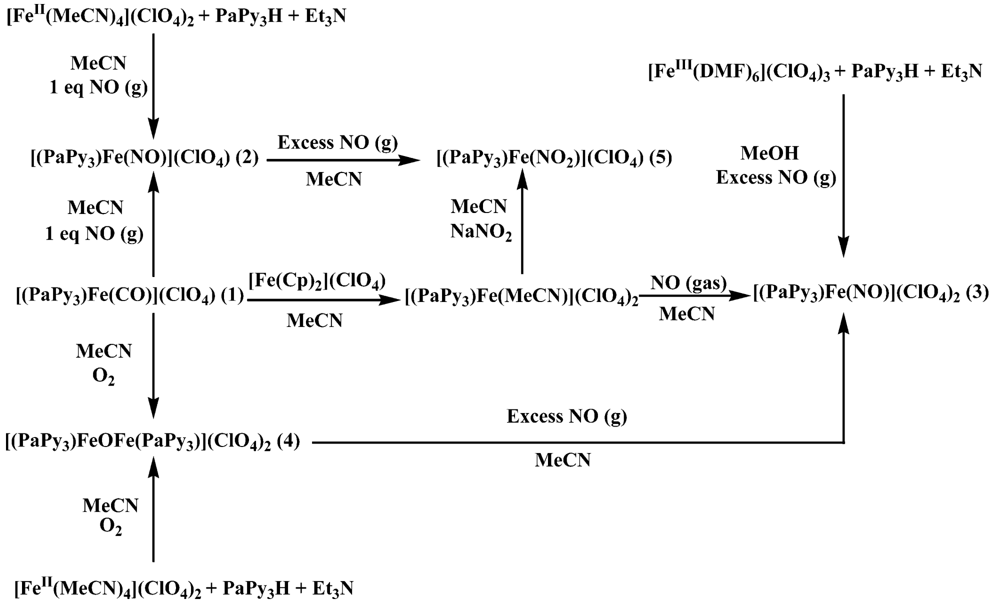

$Fe(CO)](ClO_4)\cdot 4MeOH$ (**1**·4MeOH) have been submitted as Supporting Information.

## Results and Discussion

**Syntheses and Interconversions.** The Fe(II) carbonyl **1** has been synthesized by the addition of $[Fe(MeCN)_4](ClO_4)_2$ to a mixture of $PaPy_3H$ and $Et_3N$ (1:1.1) in MeOH under strict anaerobic conditions followed by the passage of CO(g) through the red solution. Reaction of CO with the $[(PaPy_3)Fe(MeOH)]^+$ (generated in situ) results in a rapid color change to orange-red. **2** has also been synthesized by following a similar procedure and using NO (in place of CO).[18b] Complex **1** is stable in the absence of dioxygen in protic and aprotic solvents such as MeOH and MeCN. For example, **1** remains unchanged in degassed $CD_3CN$ for 96 h, as indicated by its $^1H$ NMR spectrum. Addition of 1 equiv of $Ph_3P$ under anaerobic conditions does not displace the CO ligand from **1**. However, addition of 1 equiv of NO to a solution of **1** in degassed MeCN leads to the formation of the $\{Fe-NO\}^7$ nitrosyl **2**. Clearly, the Fe(II) center in these complexes has a higher affinity toward NO compared to CO. Finally, the carbonyl complex **1** exhibits no photolability of the bound CO ligand while the corresponding isoelectronic $\{Fe-NO\}^6$ nitrosyl **3** releases NO upon exposure to low intensity visible light.[18a]

Oxidation of **1** in MeCN with 1 equiv of $[Fe(Cp)_2]^+$ results in the loss of CO and formation of the Fe(III) acetonitrile adduct $[(PaPy_3)Fe(MeCN)](ClO_4)_2$, which was previously characterized by this group.[17] The loss of CO can be followed easily by absorption spectroscopy since **1** displays its $\lambda_{max}$ at 450 nm while $[(PaPy_3)Fe(MeCN)](ClO_4)_2$ exhibits its $\lambda_{max}$ at 555 nm. When NO(g) is passed through the solution of this acetonitrile adduct, the $\{Fe-NO\}^6$ nitrosyl **3** is formed readily. These results suggest that NO has higher affinity (compared to CO) toward the Fe(III) center in $[(PaPy_3)Fe(MeCN)]^{2+}$. Indeed, $[(PaPy_3)Fe(MeCN)](ClO_4)_2$ does not react with CO in MeCN or MeOH.

Exposure of a solution of **1** in MeCN to dioxygen leads to the formation of the diiron(III) $\mu$-oxo complex **4**.[19] The displacement of CO is also facilitated by the oxidation of the Fe(II) center in this reaction. Introduction of NO to a solution of **4** affords the $\{Fe-NO\}^6$ nitrosyl **3**. This reaction resembles the reaction of the dimanganese(III) $\mu$-oxo complex $[(PaPy_3)MnOMn(PaPy_3)](ClO_4)_2$ with NO.[23] When excess NO is passed through a degassed solution of **1** in MeCN, the Fe(III) nitro complex **5**[18] is formed in good yield (∼50%). Complex **5** is also formed when excess NO is passed through a solution of the Fe(II) complex $[(PaPy_3)Fe(MeCN)](ClO_4)$ in MeCN. The color of the solution changes from red to purple-red upon passage of NO in this reaction, and the nitro complex **5** is formed within minutes. Both these reactions proceed via the formation of the $\{Fe-NO\}^7$ nitrosyl intermediate that is further attacked by excess NO to afford the nitro complex **5**. Disproportionation of NO and formation of $NO_2^-$ on a $M^{3+}$ center has been shown previously by us[24] and others.[25] However, to the best of our knowledge, the oxidative nitration of an Fe(II) center observed with a non-heme Fe(II) complex has not been reported before. All these results are summarized in Scheme 1.

**Structure of $[(PaPy_3)Fe(CO)](ClO_4)\cdot 4MeOH$ (1·4MeOH).** The structure of the Fe(II) carbonyl $[(PaPy_3)Fe(CO)]^+$ (the cation of **1**) is shown in Figure 1, and the selected bond distances and angles are listed in Table 2. The pentadentate monoanionic ligand $PaPy_3^-$ is bound to the Fe(II) center via the three pyridine nitrogens and the tertiary amine nitrogen in the equatorial plane, while the carboxamido nitrogen occupies an axial position, trans to the bound CO. This mode

---

(23) Ghosh, K.; Eroy-Reveles, A. A.; Olmstead, M. M.; Mascharak, P. K. *Inorg. Chem.* **2005**, *44*, 8469−8475.

(24) Patra, A. K.; Rose, M. J.; Olmstead, M. M.; Mascharak, P. K. *J. Am Chem. Soc.* **2004**, *126*, 4780−4781.

(25) (a) Gans, P. *J. Chem. Soc. A* **1967**, 943−946. (b) Ellison, M. K.; Schulz, C. E.; Scheidt, W. R. *Inorg. Chem.* **1999**, *38*, 100−108. (c) Franz, K. J.; Lippard, S. J. *J. Am. Chem. Soc.* **1998**, *120*, 9034−9040.

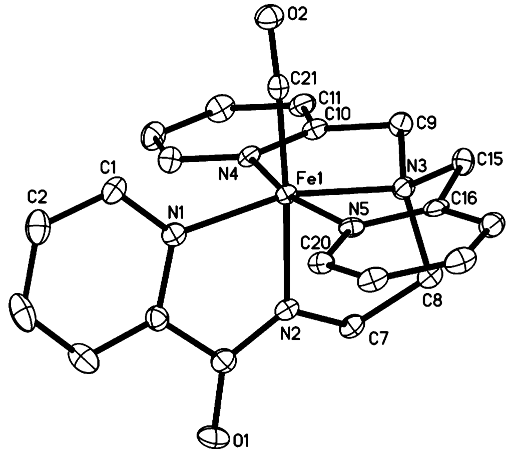

**Figure 1.** Thermal ellipsoid (probability level 50%) plot of [(PaPy$_3$)Fe(CO)]$^+$ (cation of **1**) with the atom-labeling scheme. H atoms are omitted for the sake of clarity.

of coordination of PaPy$_3$$^-$ to the iron center has been observed in **2**−**5**, as well as in other Fe(III) complexes of PaPy$_3$H.[17,18] In all cases, the carboxamido nitrogen occupies an axial position trans to the sixth exogenous ligand.

The Fe−C(O) bond distance of 1.775(3) Å of **1** lies in the range of such distances in other structurally characterized Fe(II) carbonyl {Fe−CO}$^6$ complexes (1.70−1.79 Å).[9−15] Both the short Fe−C(O) bond distance and an almost linear Fe−C(O) bond angle (176.5 (3)°) of **1** are typical of {Fe−CO}$^6$ carbonyls. The average Fe−N$_{\mathrm{Py}}$ (1.982(2) Å) and Fe−N$_{\mathrm{amine}}$ (1.997(2) Å) distances of **1** are very similar to those noted in **2** (Fe−N$_{\mathrm{Py}}$ = 1.9876(16) Å and Fe−N$_{\mathrm{amine}}$ = 1.9946(16) Å) but slightly longer than those reported in **3** (Fe−N$_{\mathrm{Py}}$ = 1.981(2) Å and Fe−N$_{\mathrm{amine}}$ = 1.972(2) Å).[18] To the best of our knowledge, this is the first structurally characterized six-coordinated {Fe−CO}$^6$ carbonyl complex that contains a carboxamido nitrogen trans to the CO ligand.

**Comparison of Structural Parameters.** The metric parameters of the equatorial plane of **1** are very similar to those of **2** and **3**.[18] However, significant differences exist along the N$_{\mathrm{amido}}$−Fe−NO(CO) vector (axial) in these three complexes. The metric parameters of the axial coordination in **1**−**3** are shown in Figure 2. Comparison of such parameters reveals that the Fe−N$_{\mathrm{amido}}$ distance (1.941(2) Å) of **1** is shorter than that of **2** (1.9577(15) Å) and longer than that of **3** (1.9009(19) Å) even though the Fe(II) carbonyl **1** and the{Fe−NO}$^6$ nitrosyl **3** are isoelectronic. The similar Fe$^{\mathrm{II}}$−C−O and Fe$^{\mathrm{III}}$−N−O bond angles of **1** and **3** (173.1(2)° and 176.5(3)°, respectively) are indicative of significant transfer of electron density from the NO ligand to the formal Fe(III) center of **3** (thus effectively an Fe(II)−NO$^+$ species). This is supported by the short Fe−N(O) distance of **3** (1.677(2) Å) as well.

The additional electron in the antibonding orbital of the NO ligand in **2** makes the N−O bond longer (1.190(2) Å) than the C−O bond in **1** (1.153(4) Å). In contrast, the Fe−N(O) bond of **2** is shorter (1.7515(16) Å) than the Fe−C(O) bond (1.775(3) Å) in **1**, an evidence of higher affinity of NO toward Fe(II) center. If one considers the three complexes **1**−**3** as Fe(II) species connected to CO, NO$^•$, and NO$^+$ respectively, then an interesting correlation is visible in Figure 2. The Fe−N$_{\mathrm{amido}}$ distances (Fe−N$_2$ distances in Figure 2) decreases in the order **2** > **1** > **3**. As the $\pi$-accepting ability of the ligand increases from NO$^•$ to CO to NO$^+$, the Fe(II) center pulls in the carboxamido nitrogen (N$_2$) closer, and hence, the Fe−N$_2$ distance keeps on decreasing in this set.

**Spectroscopic Properties**. Complex **1** displays a strong CO stretch ($\nu_{\mathrm{CO}}$) derived from the exogenous CO ligand at 1972 cm$^{-1}$, which is in the range of (1921−1980 cm$^{-1}$) noted for complexes with Fe(II)−CO bonds.[9−13,15,16] The carboxamido carbonyl stretching frequency of **1** appears at 1633 cm$^{-1}$, a fact that confirms the coordination of the deprotonated carboxamido N to the iron center ($\nu_{\mathrm{CO}}$ for free PaPy$_3$H ligand = 1666 cm$^{-1}$).[17] The $S = 0$ ground state of low-spin Fe(II) carbonyl is readily verified by the clean $^1$H NMR spectrum of this complex in degassed CD$_3$CN (Figure 3).

Much like the diamagnetic {Fe−NO}$^6$ nitrosyl **3**, the CH$_2$ group (H$_A$) of **1** gives rise to an ab pattern ($J$ = 65 and 15 Hz), while in the spectrum of the free ligand (PaPy$_3$H), these H$_A$ protons appear as a singlet. The $^{13}$C NMR spectrum of **1** in CD$_3$CN displays a chemical shift ($\delta$) of 218 ppm, which corresponds to the $^{13}$C resonance of the CO ligand. This $\delta$ value is similar to that reported by Grohman and co-workers for their Fe(II)−CO complex [(PyN$_4$)Fe(CO)]Br$_2$ (220 ppm)[15] but is much larger than those reported for the CO adducts of heme proteins[8b,26] and porphyrin-based model complexes ($\delta$ = 202−208 ppm).[11,27] The absorption spectrum of **1** in MeCN is similar to that of **2** with charge-transfer bands around ∼470 and ∼370 nm. The relative intensity and positions of these two bands of the two Fe(II) complexes **1** and **2** are distinctly different from those of the authentic Fe(III) complex **5**. In the case of the Fe(III) complex, the charge-transfer bands appear at ∼510 and ∼390 nm, whose extinction coefficients ($\epsilon$) are lower compared to those of the Fe(II) complexes.

**Redox Properties.** In MeCN, complex **1** exhibits a half-wave potential ($E_{1/2}$) of 0.215 V vs SCE (Figure 4, top). Since the CO ligand does not participate in any redox process, the voltammogram for **1** is definitely associated with the iron center. Grohman and co-workers have reported an $E_{1/2}$ value of 0.79 V (vs Fc/Fc$^+$) for the Fe(II)/Fe(III) couple of the carbonyl [(PyN$_4$)Fe(CO)]Br$_2$ in DMSO. This $E_{1/2}$ value (0.99 V vs SCE) is significantly higher than that of **1**. The facile oxidation of **1** (compared to [(PyN$_4$)Fe(CO)]Br$_2$) is, however, expected since coordination of the carboxamido nitrogen to the iron center provides more stability to the +3 oxidation state.[28] Electrochemical oxidation of the Fe(II) center of **1** in MeCN affords the Fe(III) species [(PaPy$_3$)Fe(MeCN)]$^{2+}$ (as evidenced by the color) since CO has no affinity to the Fe(III).

---

(26) (a) Moon, R. B.; Richards, J. H. *J. Am. Chem. Soc.* **1972**, *94*, 5093−5095. (b) Moon, R. B.; Richards, J. H. *Biochemistry* **1974**, *13*, 3437−3443.

(27) (a) Perkins, T.; Satterlee, J. D.; Richards, J. H. *J. Am. Chem. Soc.* **1983**, *105*, 1350−1354. (b) Matsu-ura, M.; Tani, F.; Naruta, Y. *J. Am. Chem. Soc.* **2002**, *124*, 1941−1950.

(28) Marlin, D. S.; Mascharak, P. K. *Chem. Soc. Rev.* **2000**, *29*, 69−74.

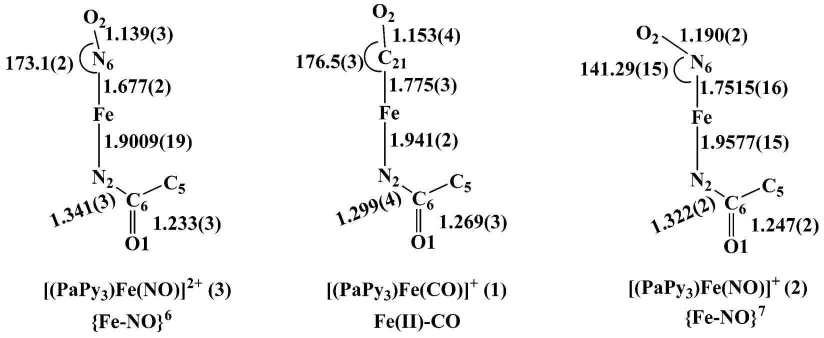

**Figure 2.** Metric Parameters of the axial coordination of **1**−**3**.

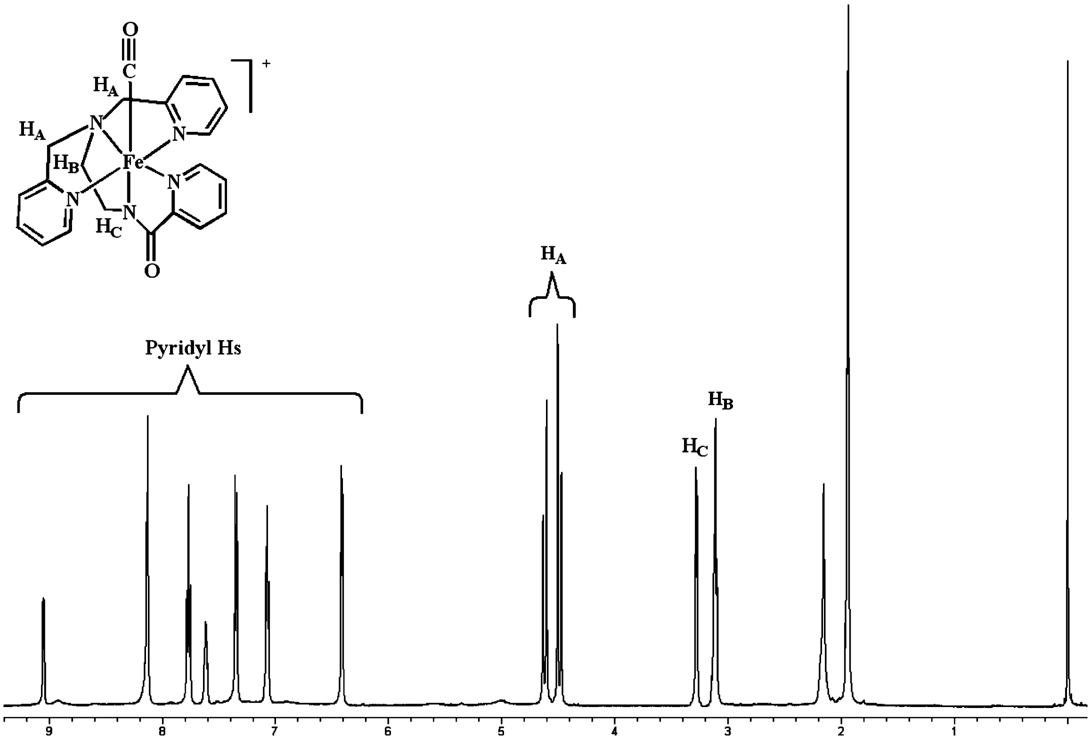

**Figure 3.** $^1$H NMR spectrum (500 MHz) of [(PaPy$_3$)Fe(CO)](ClO$_4$) (**1**) in CD$_3$CN (298 K). The two peaks at ~2 ppm represent solvent.

It is interesting to note that, in MeCN, the {Fe−NO}$^6$ nitrosyl **3** exhibits a reversible redox process with an $E_{1/2}$ value of −0.165 V (vs SCE, Figure 4, bottom). We assign this redox process to the NO/NO$^+$ couple since the same $E_{1/2}$ value (−0.165 V) is noted for another {Fe−NO}$^6$ nitrosyl (Et$_4$N)$_2$[(PhPepS)Fe(NO)] (where PhPepSH$_4$ is a tetradentate ligand with two carboxamide and two thiolate groups).[29] As reported previously, these {Fe−NO}$^6$ nitrosyls are best described as Fe(II)−NO$^+$ species,[18b,29] and hence, the initial cathodic process observed with **3** (Figure 4, bottom) arises from the NO$^+$ → NO$^\bullet$ reduction. The carbonyl complex **1**, on the other hand, exhibits an anodic process in the initial scan due to the oxidation of the Fe(II) center to Fe(III) (Figure 4, top). Our assignment is further supported by the fact that oxidation of **1** with [Fe(Cp)$_2$](ClO$_4$) affords the Fe(III) complex [(PaPy$_3$)Fe(MeCN)]$^{2+}$ (Scheme 1) while oxidation of the {Fe−NO}$^7$ nitrosyl **2** (an Fe(II)−NO$^\bullet$ species) with the same oxidant produces the {Fe−NO}$^6$ nitrosyl **3**.[18b] Clearly, in case of **1**, the redox process is metal centered, while in **2**, the redox process is NO centered.

**Mössbauer Studies.** The zero-field Mössbauer spectrum of solid **1** at 80 K shows a sharp quadrupole doublet with an isomer shift $\delta = 0.15$ mm s$^{-1}$ (relative to α-iron at room temperature) and quadrupole splitting $|\Delta E_Q| = 0.74$ mm s$^{-1}$ (Figure 5, top). The sign of the main component $V_{zz}$ of the electric field gradient tensor (efg) was determined to be negative from a magnetic spectrum recorded at 4.2 K with applied field of 5 T (Figure 5, bottom). The asymmetry parameter of the efg was found to be small, $\eta = 0.3(1)$. The magnetic hyperfine pattern could be readily simulated with zero internal magnetic field (Figure 5, bottom, solid line). This reveals a diamagnetic ground state, $S = 0$, for **1**.

The low $\delta$ and small $|\Delta E_Q|$ values are typical features of low-spin iron(II) compounds (Table 3). Examples include the ‘classical’ mono-CO adducts of the type [(Porph)Fe(base)(CO)] (Porph = various substituted porphyrinato ligands)[30] and other octahedral carbonyls derived from non-heme ligands.[15,16b,31] The small $\delta$ values in these compounds

---

(29) Harrop, T. C.; Olmstead, M. M.; Mascharak, P. K. *Inorg. Chem.* **2005**, *44*, 6918−6920.

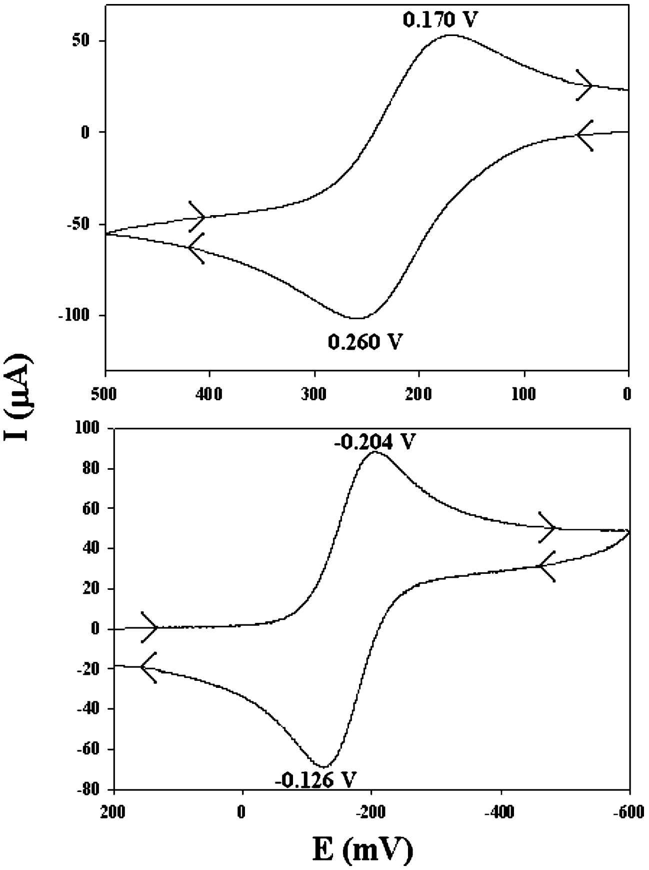

**Figure 4.** Cyclic voltammograms of the Fe(II)−CO carbonyl **1** (top) and the {Fe−NO}$^6$ nitrosyl **3** (bottom) in MeCN at 298 K. Potentials are shown vs SCE.

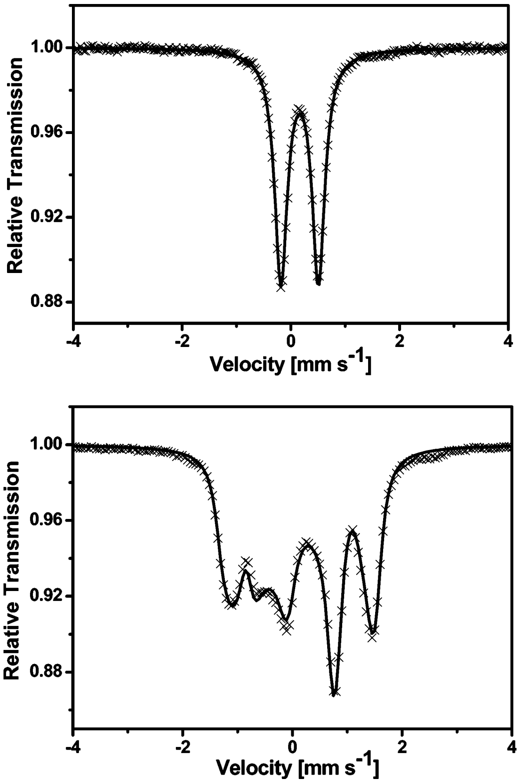

**Figure 5.** Zero-field (top) and applied field (5 T, bottom) Mössbauer spectra of solid **1** at 80 and 4.2 K, respectively.

**Table 3.** Zero-field Mössbauer Parameters of Complexes **1**−**3** and Similar Fe(II) Carbonyls and {Fe−NO}$^{6,7}$ Nitrosyls$^a$

| complex | $S$ | $\delta_{Fe}$, mm s$^{-1}$ | $\lvert\Delta E_Q\rvert$ mm s$^{-1}$ | $T$, K | ref |
|---|---|---|---|---|---|
| [(PaPy$_3$)Fe(CO)]$^+$, (**1**) | 0 | 0.16 | 0.74 | 80 | this work |
| [(PaPy$_3$)Fe(NO)]$^+$, (**2**) | 1/2 | 0.18 | 0.66 | 80 | 18b |
| [(PaPy$_3$)Fe(NO)]$^{2+}$, (**3**) | 0 | −0.05 | 0.85 | 4.2 | 18b |
| [(N$_4$Py)Fe(CO)]$^{2+}$ | 0 | 0.29 | 0.25 | 4.2 | 15 |
| [(N$_4$Py)Fe(NO)]$^{2+}$ | 1/2 | 0.31 | 0.84 | 4.2 | 15 |
| [(N$_4$Py)Fe(NO)]$^{3+}$ | 0 | 0.04 | 1.84 | 4.2 | 15 |
| [(PyS$_4$)Fe(CO)] | 0 | 0.19 | 0.88 | 298 | 16b |
| [(PyS$_4$)Fe(NO)] | 1/2 | 0.33 | 0.40 | 298 | 16b |
| [(PyS$_4$)Fe(NO)]$^+$ | 0 | 0.04 | 1.63 | 298 | 16b |
| [(TpivPP)Fe(NO$_2$)(CO)]$^+$ | 0 | 0.28 | 0.32 | 15 | 31b |
| [(TpivPP)Fe(NO$_2$)(NO)]$^-$ | 1/2 | 0.35 | 1.20 | 4.2 | 35 |
| [(TpivPP)Fe(NO$_2$)(NO)] | 0 | 0.09 | 1.43 | 4.2 | 34a |
| [(TPP)Fe(1-MeIm)(CO)] | 0 | 0.20 | 0.35 | 293 | 30b |
| [(TPP)Fe(1-MeIm)(NO)] | 1/2 | 0.35 | 0.73 | 4.2 | 34b |
| [(TPP)Fe(NO$_2$)(NO)] | 0 | 0.13 | 1.36 | 4.2 | 34a |

$^a$ Abbreviations. PyS$_4{}^{2-}$ is the anion of the pentadentate ligand 2,6-bis(2-mercaptophenylthiomethyl)pyridine; TpivPP$^{2-}$ is the anion of picket fence porphyrin; and TPP$^{2-}$ is the anion of tetrphenylporphyrin.

arise from the covalency of the Fe−CO bond and the strong $\pi$ back-bonding ability of the CO ligand.[32] This conclusion has been supported by DFT calculations in several cases.[15,16b,30b,33]

Comparison of the Mossbauer parameters of **1**−**3** (Table 3) reveals some interesting points. Results of previous studies have suggested that, in the low-spin {Fe−NO}$^7$ nitrosyl **2**, the single electron of NO is localized mainly on the NO ligand, i.e., the nitrosyl is best described as an Fe(II)−NO$^\bullet$ species.[18b] This is now further supported by the Mössbauer data of **1**, a genuine Fe(II) species. The $\delta$ values of **1** and **2** are very close to each other, and the $\Delta E_Q$ values are also both small and similar in their absolute values (the signs are opposite, however). When the Mössbauer parameters of **3** are compared with those of **1** and **2**, one also obtains support for its Fe(II)−NO$^+$ description.[18b] On the basis of the results of Mössbauer and theoretical studies on a series of iron complexes of the type [(PyS$_4$)Fe(X)]$^{n+}$ (X = NO, CO, NO$^+$), Weighardt and co-workers have recently suggested that the $\delta$ and $\Delta E_Q$ values in such species depend critically on the $\pi$-accepting ability of the X ligand.[16b] When X is a relatively weak $\pi$-acceptor, the resulting complex should exhibit larger $\delta$ and smaller $\Delta E_Q$ values compared to a similar Fe(II) complex with a stronger $\pi$-acceptor X ligand. In the present work, we notice this trend. The $\delta$ and $\Delta E_Q$ values of **1** are, respectively, smaller and larger compared to those values

---

(30) (a) Collman, J. P.; Gagne, R. R.; Reed, C. A.; Halbert, T. R.; Lang, G.; Robinson, W. T. *J. Am. Chem. Soc*. **1975**, *97*, 1427−1439. (b) Havlin, R. H.; Godbout, N.; Salzmann, R.; Wojdelski, M.; Arnold, W.; Schulz, C. E.; Oldfield, E. *J. Am. Chem. Soc*. **1998**, *120*, 3144−3151.

(31) (a) Sellman, D.; Soglowek, W.; Knoch, F.; Ritter, G.; Dengler, J. *Inorg. Chem*. **1992**, *31*, 3711−3717. (b) Nasri, H.; Ellison, M. K.; Shang, M.; Schulz, C. E.; Scheidt, W. R. *Inorg. Chem*. **2004**, *43*, 2932−2942.

(32) Dannon, J. In *Chemical Applications of Mössbauer Spectroscopy*; Goldanski, V. I., Herber, R. H., Eds.; Academic Press: New York, 1968; pp 160−267.

(33) Neese, F. *Inorg. Chim. Acta* **2002**, *337*, 181−192.

(34) (a) Ellison, M. K.; Schulz, C. E.; Scheidt, W. R. *Inorg. Chem*. **1999**, *38*, 100−108. (b) Wyllie, G. R. A.; Schulz, C. E.; Scheidt, W. R. *Inorg. Chem*. **2003**, *42*, 5722−5734.

(35) Nasri, H.; Ellison, M. K.; Chen, S.; Huynh, B. H.; Scheidt, W. R. *J. Am. Chem. Soc*. **1997**, *119*, 6274−6283.

of **2**. This clearly indicates that $NO^\bullet$ is a weaker $\pi$-acceptor compared to CO. It is interesting to note that the $\{Fe-NO\}^6$ nitrosyl **3**, an effectively Fe(II)$-NO^+$ species,[18b] exhibits the smallest $\delta$ ($-0.05$ mm s$^{-1}$) and largest $\Delta E_Q$ (0.85 mm s$^{-1}$) value in the series **1**−**3**. The $\pi$-accepting ability of $NO^+$, $NO^\bullet$, and CO therefore follows the trend $NO^+ > CO > NO^\bullet$. Weighardt and co-workers have noted the same trend (Table 3) in their work with $[(PyS_4)Fe(X)]^{n+}$ (X = $NO^+$, CO, $NO^\bullet$).[16b]

**Summary and Conclusions.** The following are the summary and conclusions of the present work.

(1) The Fe(II) carbonyl complex of the pentadentate polypyridine ligand $PaPy_3H$, namely **1**, has been isolated and structurally characterized.

(2) In degassed MeCN, this diamagnetic carbonyl readily reacts with 1 equiv of NO to form the $\{Fe-NO\}^7$ nitrosyl **2**. Clearly, NO has higher affinity toward the $\{(PaPy_3)Fe(II)\}$ moiety compared to CO. Reactions of excess NO with **1**, however, affords the Fe(III) nitro complex **5**. The conversion **1** → **5** is the first example of an Fe(II) center undergoing in situ oxidative nitration by NO.

(3) In the presence of $[Fe(Cp)_2]^+$, reaction of **1** with excess NO in MeCN leads to the formation of the $\{Fe-NO\}^6$ nitrosyl **3** via the intermediacy of $[(PaPy_3)Fe(MeCN)]^{2+}$.

(4) Although NO in the $\{Fe-NO\}^6$ nitrosyl **3** is photolabile, **1** exhibits no photolability of CO. In this regard, **1** resembles the $\{Fe-NO\}^7$ nitrosyl **2**. Also, like **2**, complex **1** readily reacts with dioxygen to afford the diiron(III) $\mu$-oxo complex **4**.

(5) In a previous account, the $\{Fe-NO\}^{6,7}$ nitrosyls **3** and **2** were described as complexes containing Fe(II)$-NO^+$ and Fe(II)$-NO^\bullet$ units, respectively.[18b] Comparison of the spectral properties of **1**−**3** confirms these assignments. For example, the isomer shift ($\delta$) and quadrupole splitting ($\Delta E_Q$) parameters of these species are close to each other (Table 3). This similarity attests that all three complexes are effectively Fe(II) species. However, further scrutiny of the Mössbauer parameters reveals that $NO^\bullet$ is a weaker $\pi$-acceptor compared to CO and the $\pi$-accepting ability of $NO^+$, $NO^\bullet$, and CO follows the trend $NO^+ > CO > NO^\bullet$.

(6) In solvents such as MeCN, electrochemical oxidation of **2** leads to **3** in which the coordinated NO loses one electron (the iron center remains in +2 oxidation state). In contrast, **1** exhibits redox activity associated with the metal center and affords the Fe(III) species $[(PaPy_3)Fe(MeCN)]^{2+}$.

**Supporting Information Available:** X-ray crystallographic data (in CIF format) and tables for the structure determination of $[(PaPy_3)Fe(CO)](ClO_4)\cdot 4MeOH$ (**1**·4MeOH). This material is available free of charge via the Internet at http://pubs.acs.org.

IC060020N